

High-spin study of ^{162}Ta

F. Ghazi Moradi,^{1,*} T. Bäck,¹ B. Cederwall,¹ M. Sandzelius,^{1,†} A. Atac,^{1,‡} A. Johnson,¹ C. Qi,¹ R. Liotta,¹ B. Hadinia,^{1,§} K. Andgren,¹ A. Khaplanov,^{1,||} R. Wyss,¹ S. Eeckhaudt,² T. Grahn,² P. T. Greenlees,² P. M. Jones,² R. Julin,² S. Juutinen,² S. Ketelhut,² M. Leino,² M. Nyman,² P. Rahkila,² J. Sarén,² C. Scholey,² J. Sorri,² J. Uusitalo,² E. Ganioglu,³ J. Thomson,⁴ D. T. Joss,⁴ R. D. Page,⁴ S. Ertürk,⁵ J. Simpson,⁵ M. B. Gomez Hornillos,⁶ and L. Bianco⁷

¹Royal Institute of Technology, SE-10691 Stockholm, Sweden

²Department of Physics, University of Jyväskylä, FIN-40014 Jyväskylä, Finland

³Science Faculty, Physics Department, Istanbul University, 34134 Istanbul, Turkey

⁴Oliver Lodge Laboratory, University of Liverpool, Liverpool L69 7ZE, United Kingdom

⁵CCLRC Daresbury Laboratory, Daresbury, Warrington WA4 4AD, United Kingdom

⁶Seccio d'Enginyeria Nuclear, Universitat Politècnica de Catalunya, E-08028 Barcelona, Spain

⁷Department of Physics, University of Guelph, 50 Stone Road East, Guelph, Ontario N1G 2W1, Canada

(Received 11 October 2011; published 13 December 2011)

Excited states in the odd-odd neutron deficient nucleus ^{162}Ta ($Z = 73$, $N = 89$) have been studied for the first time. The gamma spectroscopy analysis using $\gamma - \gamma - \gamma$ coincidences revealed a strongly coupled rotational structure that was established up to large angular momentum states. The rotational band was assigned to the configuration $\pi h_{11/2}[514]9/2 \otimes \nu i_{13/2}[660]1/2$ based on its rotational and electromagnetic properties. The data are interpreted within the framework of total Routhian surface calculations, which suggests an axially symmetric shape with a γ -soft minimum at $\beta_2 \approx 0.16$ and $\gamma \approx 6^\circ$. The crossing of the signature partners observed in heavier ($N \geq 91$) odd-odd nuclides in this mass region is found to be absent at $N = 89$. This might be correlated with a change in S -band structure above the paired band crossing at these neutron numbers.

DOI: [10.1103/PhysRevC.84.064312](https://doi.org/10.1103/PhysRevC.84.064312)

PACS number(s): 21.10.Re, 21.10.Pc, 25.70.-z, 27.70.+q

I. INTRODUCTION

Recent studies of the odd-odd nuclides in the $Z \approx 70$, $A \approx 160$ – 170 region of the nuclide chart have revealed several interesting phenomena originating from the delicate interplay between the odd valence neutron and proton as well as with a deformation-soft core. Most of these neutron deficient nuclei are predicted by theory to be deformed in the ground state, typically with a near-prolate shape at $\beta_2 \approx 0.2$, and a large set of rotational band structures built on different quasiparticle configurations have been experimentally established in the region. One of the questions of interest in these structures is the energy splitting between the two signatures in strongly coupled bands built on high- j single-particle configurations and how it varies with angular momentum. For the Ta isotopes, significant signature splitting has been observed in the yrast rotational bands of both the odd- A [built on the $\pi h_{11/2}$ quasiparticle (qp) configuration] and even- A (built on the $\pi h_{11/2} \otimes \nu i_{13/2}$ qp configuration) isotopes [1–5] and is usually believed to be associated with triaxial shapes induced by the deformation-driving properties of the $\pi h_{11/2}$ and $\nu i_{13/2}$ single particle orbitals. A striking phenomenon observed in

the region is the *signature inversion* in the yrast band of some odd-odd $A \approx 160$ nuclides [6–9]. This phenomenon has been studied using various theoretical approaches [10–15], and several attempts have been made to explain its origin. For example, the connection between triaxiality and signature inversion was discussed in Refs. [10,11], the influence of the neutron-proton residual interaction on signature inversion was investigated in Ref. [12], while quadrupole pairing was proposed as a possible origin of “anomalous” signature splitting in Ref. [15]. However, a consistent theoretical explanation is so far lacking.

In this work we report on the observation of excited states of the neutron deficient nuclide ^{162}Ta . The data analysis revealed a strongly coupled $E2/M1$ band structure reaching an angular momentum of approximately $30\hbar$. The configuration assignment is discussed in terms of the experimentally deduced electromagnetic and rotational properties of the band and compared with neighboring nuclei in the framework of the cranked shell model (CSM) and total Routhian surface (TRS) calculations. The systematics of the signature inversion phenomenon are also discussed by comparing with a few adjacent odd-odd nuclei in the region.

II. EXPERIMENTAL DETAILS AND DATA ANALYSIS

The ^{162}Ta nuclei were produced using the $^{106}\text{Cd}(^{60}\text{Ni}, 3\text{pn})$ fusion-evaporation reaction at a beam energy of 270 MeV. The experiment was performed at the accelerator laboratory at the University of Jyväskylä, using the K130 cyclotron. The beam was focused on a self-supporting target foil of enriched ^{106}Cd with a thickness of $500 \mu\text{g}/\text{cm}^2$. Coincident γ -ray events were recorded at the target position by the JUROGAM γ -ray

*farnazg@kth.se

†Present address: Department of Physics, University of Jyväskylä, FIN-40014 Jyväskylä, Finland.

‡Present address: Department of Physics, Ankara University, 06100 Tandoğan, Ankara, Turkey.

§Present address: Department of Physics, University of Guelph, 50 Stone Road East, Guelph, Ontario N1G 2W1, Canada.

||Present address: European Spallation Source AB, P.O. Box 176, SE-221 00 Lund, Sweden.

spectrometer [16] consisting of 43 Compton-suppressed HPGe detectors situated in an array of six rings at different angles relative to the beam. The total photopeak efficiency was 4.2% at 1.3 MeV. The separation of recoiling fusion-evaporation products from scattered beam particles and fission products was performed by the gas-filled recoil separator Recoil Ion Transport Unit (RITU) [17,18]. The reaction products were subsequently implanted at the focal plane of RITU into the double-sided silicon strip detector (DSSD) of the spectrometer Gamma Recoil Electron Alpha Tagging (GREAT) [19]. This composite detector installation additionally consists of a multiwire proportional counter (MWPC), an array of Si PIN diode detectors, a planar germanium detector, and two high-efficiency segmented clover-type Ge detectors. A triggerless total data readout (TDR) acquisition system [20] with a 10-ns time-stamp precision was used for collecting data. The events were then reconstructed offline using the GRAIN software package [21]. In the off-line analysis, only events with a recoil implantation signal in the DSSD of the focal plane were selected. A narrow time gate was defined to select prompt coincidences between any of the JUROGAM Ge detectors and the events were then sorted into two-dimensional and three-dimensional γ -ray energy histograms. In the off-line analysis, the LEVIT8R code from the RADWARE software package [22] was used to construct the level scheme. For the multipolarity assignment the angular intensity ratios of the strongest γ -ray transitions were obtained using the method of directional correlations from oriented states (DCO).

III. LEVEL SCHEME

The resulting level scheme for ^{162}Ta presented in Fig. 1 shows a rotational band structure with two signatures featuring strong $\Delta I = 1$ transitions as well as $E2$ crossover transitions. The ordering of the γ -rays was obtained from coincidence relationships and relative intensities. The assignment of the band structure to atomic number $Z = 73$ is based on the coincidences between clean in-band transitions and characteristic tantalum x rays whereas a majority of the γ -rays in the level scheme have been assigned to mass $A = 162$ in a previous mass spectrometer study [23]. Hence, the deduced level structure is unambiguously assigned to the nuclide ^{162}Ta . Figure 2 shows two representative double coincidence spectra. The spin assignments of the energy levels are based on the DCO ratios and the systematic comparisons of heavier odd-odd Ta isotopes. The coincidences between the detector rings at 94° and 158° were sorted into a matrix with 94° along one axis and 158° along the other axis. The corresponding experimental DCO ratio can be extracted as

$$R_{\text{DCO}} = \frac{I_{\gamma_2}^{\theta_1}(\text{gated by } \gamma_1 \text{ at } \theta_2)}{I_{\gamma_2}^{\theta_2}(\text{gated by } \gamma_1 \text{ at } \theta_1)}. \quad (1)$$

Setting a gate on a clean $E2$ -type transition γ_1 , it is then expected that $R_{\text{DCO}} \sim 0.8$ if γ_2 is a stretched dipole transition and that $R_{\text{DCO}} \sim 1$ if γ_2 is a stretched $E2$ transition. For the weakly populated levels at high spins, R_{DCO} values could not be determined due to poor statistics. It was also not possible to

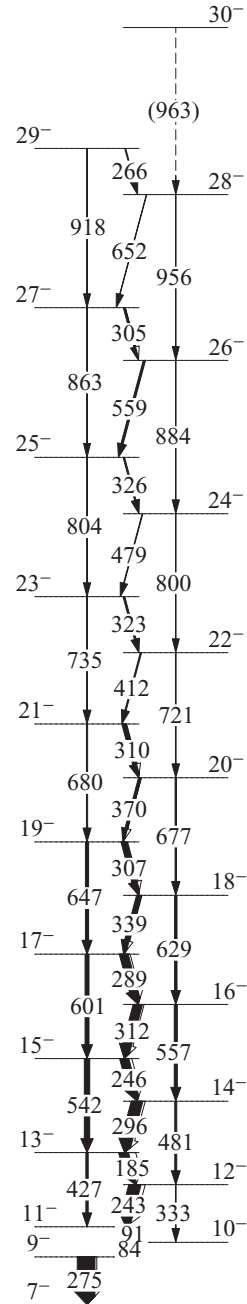


FIG. 1. Proposed level scheme for ^{162}Ta . Energies are given in keV. All spin and parity assignments are tentative. The relative widths of the arrows indicate the transition intensities.

measure the multipole character of the highly converted 84 keV γ -ray. The placement of the 275 keV transition as populating the lowest-lying state in the proposed level scheme is based on its presence in all of the double-gate combinations in coincident spectra and its high relative intensity. Based on the excitation energy systematics of the odd-odd Ta isotopes [1], the spin and parity of the bandhead was tentatively assigned as 9^- . The energies, relative intensities and R_{DCO} values for the γ -rays assigned to ^{162}Ta are listed in Table I.

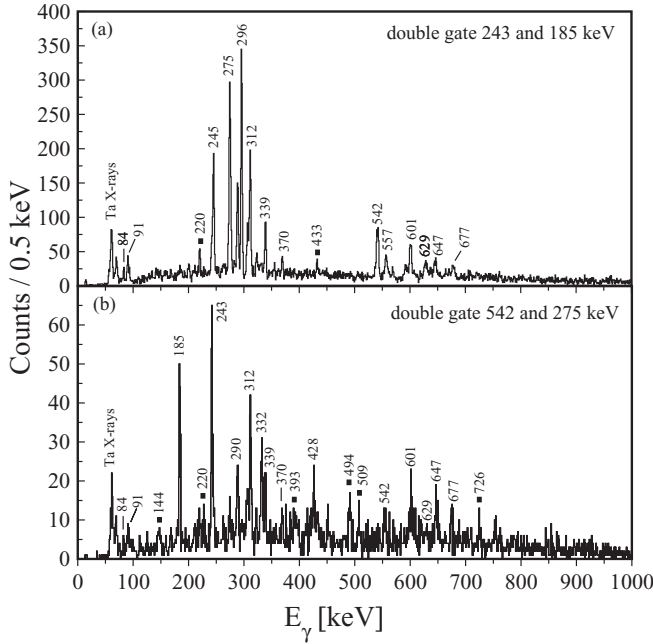


FIG. 2. Sample spectra obtained in the $\gamma\gamma\gamma$ analysis of ^{162}Ta . The filled squares indicate γ -rays assigned to ^{163}Ta .

IV. BAND ASSIGNMENT AND DISCUSSION

The configuration assignment for the rotational band structure in ^{162}Ta is based on the systematics of the low-lying single-particle states in the neighboring odd- A nuclei together with the observed aligned angular momentum, $B(M1)/B(E2)$ ratios, and signature splitting behavior. With a prolate deformation of $\beta_2 \approx 0.16$ given by our TRS calculation the most relevant Nilsson orbitals close to the Fermi surface in ^{162}Ta emanate from the $i_{13/2}$, $h_{9/2}$, and $f_{7/2}$ neutron subshells and the $h_{11/2}$, $d_{5/2}$, and $g_{7/2}$ proton subshells. The low-spin parts of the yrast bands in $^{161,163}\text{Ta}$ [3,4] have been assigned to $\pi h_{11/2}[514]9/2^-$, whereas the yrast band of $^{161,163}\text{Hf}$ are known to be built on the $\nu i_{13/2}[660]1/2^-$ state [24,25]. In accordance with the Gallagher-Moszkowski rule [26] we propose that the parallel coupling of the valence particle angular momenta lies lower in energy than the antiparallel coupling at the bandhead in this odd-odd nucleus (i.e., a likely scenario is that the ^{162}Ta yrast band is built on a configuration where a high- Ω $\pi h_{11/2}$ proton is coupled with a low- Ω $\nu i_{13/2}$ neutron with a resulting band head angular momentum and parity 9^-). Similar yrast configurations have been observed in other neighboring odd-odd $Z = 73$ isotopes [1,5,27] and $N = 89$ ^{158}Tm and ^{160}Lu isotones [28,29].

Analyzing its rotational properties provides further insights into the structure of the band. The total experimental Routhians (energies in the rotating frame of the nucleus) are obtained by subtracting a reference rotor from the measured level energies. The degree of quasiparticle alignment can be observed in the plot of aligned angular momentum i versus rotational frequency with respect to the same reference rotor. The total experimental Routhians e' and alignments i are, respectively, expressed by

$$e'(\omega) = E'(\omega) - \omega I_x(\omega) - E_{\text{ref}}(\omega) \quad (2)$$

TABLE I. γ -ray transition energies, intensities, DCO ratios, and tentative spin/parity assignments in ^{162}Ta . Statistical uncertainties of energies and intensities are given in parentheses. All intensities are normalized to the 243 keV transition.

E_γ (keV)	I_γ (%)	R_{DCO}	$J_i^\pi \rightarrow J_f^\pi$
275.4(0)	123.6(52)	1.24(12)	$9^- \rightarrow 7^-$
84.0(10)	6.6(16)		$10^- \rightarrow 9^-$
90.6(0)	13.9(19)	0.67(23)	$11^- \rightarrow 10^-$
332.6(10)	4.9(17)	1.28(13)	$12^- \rightarrow 10^-$
242.7(0)	100.0(45)	0.83(6)	$12^- \rightarrow 11^-$
427.2(2)	19.0(19)	0.90(34)	$13^- \rightarrow 11^-$
184.5(0)	80.9(31)	0.77(8)	$13^- \rightarrow 12^-$
481.2(2)	16.3(17)	1.06(35)	$14^- \rightarrow 12^-$
296.4(0)	95.1(36)	0.78(9)	$14^- \rightarrow 13^-$
541.8(1)	45.1(26)	1.0(30)	$15^- \rightarrow 13^-$
245.6(0)	75.0(30)	1.0(13)	$15^- \rightarrow 14^-$
556.7(2)	25.7(26)	1.07(35)	$16^- \rightarrow 14^-$
312.4(0)	76.5(30)	0.89(11)	$16^- \rightarrow 15^-$
601.3(1)	32.8(27)	1.41(61)	$17^- \rightarrow 15^-$
289.4(0)	72.9(30)	0.97(10)	$17^- \rightarrow 16^-$
628.8(2)	20.3(22)	1.07(28)	$18^- \rightarrow 16^-$
339.4(1)	39.1(20)	0.89(33)	$18^- \rightarrow 17^-$
646.7(1)	26.3(25)	1.10(23)	$19^- \rightarrow 17^-$
307.3(0)	45.7(21)	0.89(14)	$19^- \rightarrow 18^-$
676.8(2)	11.6(15)		$20^- \rightarrow 18^-$
369.8(1)	21.5(16)	0.79(34)	$20^- \rightarrow 19^-$
679.9(3)	9.6(17)		$21^- \rightarrow 19^-$
310.3(1)	33.4(17)		$21^- \rightarrow 20^-$
721.3(3)	5.4(14)		$22^- \rightarrow 20^-$
412.0(1)	9.6(13)	0.84(36)	$22^- \rightarrow 21^-$
735.5(3)	7.7(14)		$23^- \rightarrow 21^-$
322.8(1)	12.8(14)		$23^- \rightarrow 22^-$
800.4(4)	2.1(9)		$24^- \rightarrow 22^-$
478.8(1)	5.3(12)		$24^- \rightarrow 23^-$
804.3(4)	2.8(10)		$25^- \rightarrow 23^-$
325.7(1)	10.6(12)		$25^- \rightarrow 24^-$
883.5(6)	2.3(10)		$26^- \rightarrow 24^-$
559.3(1)	17.7(17)		$26^- \rightarrow 25^-$
862.7(10)	1.3(10)		$27^- \rightarrow 25^-$
305.0(1)	14.4(12)		$27^- \rightarrow 26^-$
956.1(16)	0.4(7)		$28^- \rightarrow 26^-$
652.0(2)	3.8(18)		$28^- \rightarrow 27^-$
918.0(11)	2.0(9)		$29^- \rightarrow 27^-$
266.0(2)	6.1(7)		$29^- \rightarrow 28^-$
963.0(10)	0.3(9)		$30^- \rightarrow 28^-$

and

$$i(\omega) = I_x(\omega) - I_{\text{ref}}(\omega). \quad (3)$$

Here $I_x(\omega)$ is the projection of angular momentum along the rotational axis x and $E'(\omega)$ is obtained from the energy at the intermediate value of the angular momentum I . The angular momentum and energy, as a function of rotational frequency, for the reference configuration in the Harris description [30] are

$$I_{\text{ref}}(\omega) = (\mathcal{J}_0\omega + \mathcal{J}_1\omega^3) \quad (4)$$

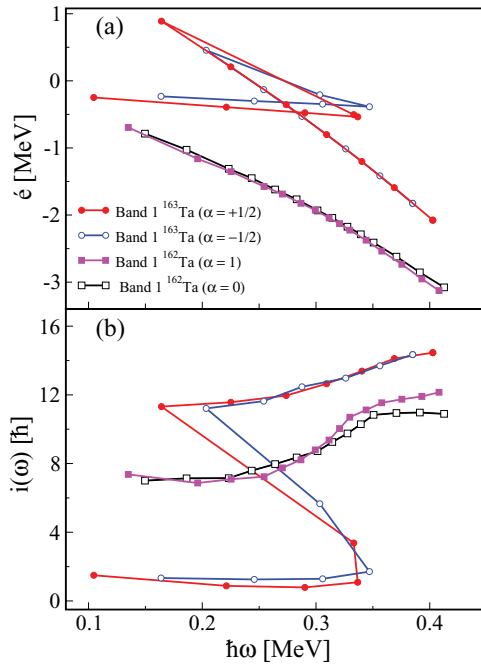


FIG. 3. (Color online) (a) Experimental Routhians for the rotational band assigned to ^{162}Ta . (b) Aligned angular momenta versus rotational frequency in ^{162}Ta and ^{163}Ta [4]. The open (solid) symbols refers to favored (unfavored) signatures.

and

$$E_{\text{ref}}(\omega) = \frac{1}{8\mathcal{J}_0} - \frac{\omega^2}{2}\mathcal{J}_0 - \frac{\omega^4}{4}\mathcal{J}_1. \quad (5)$$

Adopting $I^\pi = 7^-$ for the spin-parity of the lowest observed state in ^{162}Ta , the extracted experimental Routhians and quasiparticle alignments versus rotational frequency are compared with ^{163}Ta in Fig. 3. To obtain an approximately constant alignment at low rotational frequencies and to test the additivity of alignments of neighboring odd- A nuclei the same set of Harris parameters ($J_0 = 21\hbar^2 \text{ MeV}^{-1}$ and $J_1 = 63\hbar^4 \text{ MeV}^{-3}$) was chosen as for ^{162}Hf , ^{161}Hf , and ^{163}Ta [4,25]. At low rotational frequencies ($\hbar\omega = 0.2 \text{ MeV}$) the observed initial alignment ($\approx 7\hbar$) is found to be consistent with similar observations in the neighboring $^{164,166}\text{Ta}$ nuclei. The alignment is similar to the sum of alignments of the yrast configuration of the neighboring odd- Z ^{163}Ta ($\approx 2\hbar$) [4] and odd- N ^{161}Hf ($\approx 4\hbar$) [24] nuclides. The band in ^{162}Ta undergoes an alignment gain of $\Delta i \approx 4\hbar$ at $\hbar\omega = 0.3 \text{ MeV}$, which is delayed by about 0.05 MeV with respect to the observed band crossing frequency in ^{163}Ta due to the alignment of a pair of $i_{13/2}$ quasineutrons. This is consistent with the odd $i_{13/2}$ neutron in ^{162}Ta blocking the first alignment at this frequency leading to a delayed alignment of the second and the third lowest quasineutrons (BC crossing). However, at $N = 89$, the neutron Fermi level is significantly below the $i_{13/2}$ subshell and neutron two-qp alignments emanating from the mixed $f_{7/2}$ and $h_{9/2}$ spherical subshells can compete with the pure $i_{13/2}$ two-quasineutron alignment [3]. Paired band crossings involving four-qp configurations based on different combinations of the $f_{7/2}$, $h_{9/2}$, and $i_{13/2}$ subshells are predicted by our cranked shell

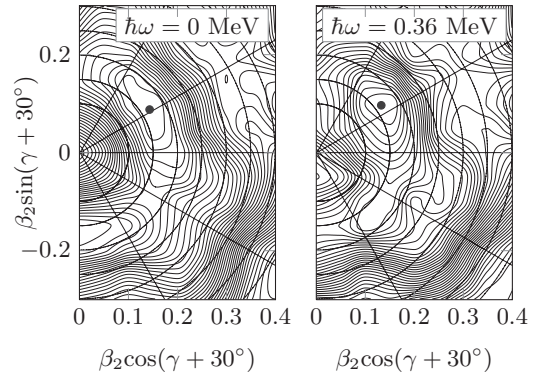


FIG. 4. The total Routhian surfaces of ^{162}Ta for the configuration proton $(\pi, \alpha) = (-, -1/2) \otimes$ neutron $(\pi, \alpha) = (+, +1/2)$. At $\omega = 0$ there is a minimum at prolate shape near $\beta_2 \approx 0.16$. After the band crossing at $\hbar\omega = 0.36 \text{ MeV}$ the minimum shifts to a slightly triaxial shape with $\gamma \approx 6^\circ$. The energy step between contour curves is 200 keV.

model calculations at similar rotational frequencies as that due to the $\nu(i_{13/2})^2$ alignment. It is interesting to note how the two signature partners of the ^{162}Ta band are separated in energy above $\hbar\omega = 0.35 \text{ MeV}$ in a way so that the $\alpha = 0$ branch does not show any indication of a second alignment while the $\alpha = 1$ signature partner band exhibits an increase in the aligned angular momentum starting at $\hbar\omega \approx 0.35 \text{ MeV}$. This suggests that this second band crossing has a proton character. The total Routhian surface minima for the two-quasiparticle configuration in the ground state and the four-quasiparticle configuration at $\hbar\omega = 0.36 \text{ MeV}$ are shown in Fig. 4.

The quasiparticle configuration of the rotational structure observed in ^{162}Ta can be further tested by comparing experimental $B(M1)/B(E2)$ ratios deduced from the relative γ -ray intensities with theoretical calculations based on the geometrical model of Dönau and Frauendorf [31,32]. In these calculations a quadrupole moment of $Q_0 = 3.9 \text{ eb}$ was adopted based on the deformation parameters obtained from the total Routhian surface calculations. Other parameters used for the calculations are summarized in Table II. The results shown in Fig. 5 indicate that only the $\pi h_{11/2} \otimes \nu i_{13/2}$ two-qp configuration is in good agreement with the experimental values below the band crossing at $\hbar\omega = 0.36 \text{ MeV}$. The transition between the two-qp and four-qp configurations is taken into account according to the predictions from our cranked shell model calculations.

The favored signature of a high- j configuration in odd-odd nuclei is defined as [11]

$$\alpha_f = \frac{1}{2}[(-1)^{j_p - \frac{1}{2}} + (-1)^{j_n - \frac{1}{2}}]. \quad (6)$$

This means that for $\pi h_{11/2}$ and $\nu i_{13/2}$ we would expect that the even-spin Routhian should lie lower in energy. However, based on our tentative spin assignments, Fig. 3 shows that the experimental Routhians of the $\alpha = 1$ signature (odd-spins) is lower in energy than the $\alpha = 0$ signature (even spins). Such an inversion of signature at low spins has been claimed for several neutron deficient rare-earth nuclides [6–9,27] but its underlying mechanism is not well

TABLE II. Parameters used for theoretical Dönau and Frauendorf $B(M1)/B(E2)$ ratios shown in Fig. 5. The parameters i and i^c denote alignment values before and after the crossing frequency, respectively.

Configuration	g_Ω	Ω	$i(\hbar)$	$i^c(\hbar)$
$\pi h_{11/2} \otimes \nu i_{13/2}$	1.3	4.5	1.6	—
$\pi d_{5/2} \otimes \nu i_{13/2}$	1.4	2.5	0.0	—
$\pi g_{7/2} \otimes \nu i_{13/2}$	0.70	3.5	0.0	—
$\nu(f_{7/2}, h_{9/2})$	-0.17	1.5	1.6	2.7
$\nu(i_{13/2})^2$	-0.32	0.5	1.6	5.0

understood. It is, however, worth pointing out that solid spin-parity assignments are often lacking in these studies. However, our spin assignments, in particular the assignment of signature to the observed rotational states, are in accordance with the experimentally deduced $B(M1)/B(E2)$ ratios, which supports the suggestion that the energy splitting between the signature partners really is inverted throughout the yrast band of ^{162}Ta . It is illustrative to compare the signature properties of the yrast bands in the region in terms of the energy staggering, defined as

$$S(I) = E(I) - \frac{1}{2}[E(I+1) - E(I-1)]. \quad (7)$$

The energy staggering between the two signatures was deduced for eight odd-odd isotopes and isotones in the neighborhood of ^{162}Ta , see Fig. 6. For these three isotopic chains one can first observe that the amplitude of the energy staggering increases with decreasing neutron number, at least for spins up to $20\hbar$.

For each of the three $N = 93$ isotones, there is a point where the two signature partners cross each other. This inversion point seems to move upward in spin for increasing proton number. The same effect is seen for the $N = 91$ isotones. For $N = 89$, however, the situation is dramatically different, with no observed crossing of signatures. The point of inversion is

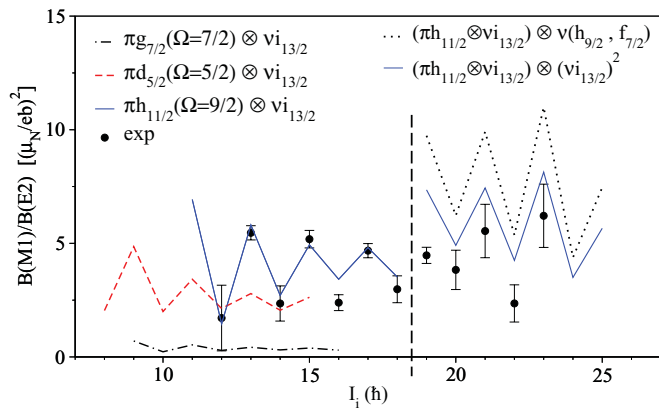


FIG. 5. (Color online) Experimental and theoretical $B(M1)/B(E2)$ values for the strongly coupled bands in ^{162}Ta plotted as a function of initial spin I_i . The dashed line separates different two-qp and four-qp configurations, respectively, before and after the paired band crossing.

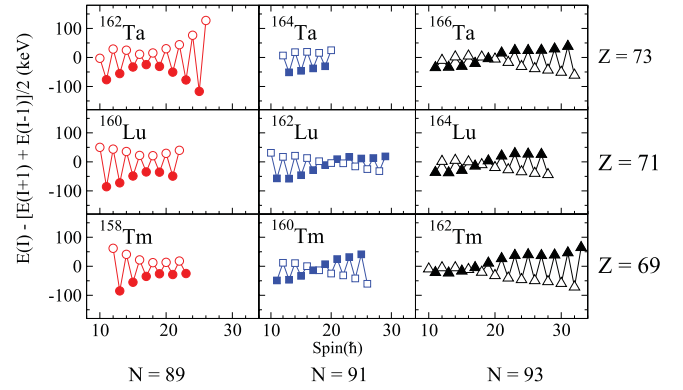


FIG. 6. (Color online) Comparison of energy staggering (in units of keV) between the $\alpha = 0$ and $\alpha = 1$ signatures for $\pi h_{11/2} \nu i_{13/2}$ bands in odd-odd rare-earth nuclei in the neighborhood of ^{162}Ta . The open symbols correspond to the signature that is expected to be favored according to Eq. (6). Data are taken from Refs. [1,5,28,29,33–35].

here replaced by a minimum in the amplitude of $S(I)$. This effect is more pronounced in ^{162}Ta compared to ^{160}Lu and ^{158}Tm . We note that this change in the staggering behavior between $N = 89$ and $N = 91$ coincides with the proposed shape phase transition in rare-earth nuclei at $N = 90$ as recently discussed by Casten [36]. The two signature partners of the $\pi h_{11/2} \otimes \nu i_{13/2}$ configuration are generated by coupling the $\alpha = +1/2$ signature of the $\nu i_{13/2}$ orbital to both signature partners of the $\pi h_{11/2}$ orbital. While the $\pi h_{11/2}$ yrast bands of the neighboring $^{161,163}\text{Ta}$ isotopes [3,4] both exhibit a large signature staggering of around $S = \pm 200$ keV below the paired band crossing the corresponding staggering values for ^{162}Ta are much smaller and lie in the range $S = \pm 50$ keV. This is consistent with the core polarization effect of the additional $i_{13/2}$ valence neutron, counteracting the triaxial shape-driving effect of the $\pi h_{11/2}$ orbital and driving the nucleus back toward a prolate shape. In all three isotopes the staggering amplitude reaches a minimum close to the band crossing. But while the staggering amplitude essentially vanishes above the assigned $\nu(i_{13/2})^2$ band crossing in ^{163}Ta and heavier Ta odd-even isotopes, ^{161}Ta exhibits an *increase* in staggering amplitude after its minimum value. This was associated by Lagergren *et al.* [3] with an alignment of a more weakly shape-polarizing pair of mixed-character $f_{7/2}, h_{9/2}$ neutrons. A similar, but less pronounced effect is observed in ^{162}Ta while in the heavier odd-odd $^{166,168}\text{Ta}$ isotopes [5,27] the staggering pattern (i.e., the signature splitting is *reversed* after the band crossing). Hence, it appears that the change in the signature inversion pattern for $N = 89$ might be associated with the character of the S band, after the crossing. It is noteworthy that these findings are difficult to reconcile with the results of our TRS calculation, which do not predict large differences in the nuclear shapes as the neutron number decreases along the Ta isotopic chain. Although numerous and diverse attempts (e.g., based on strong residual neutron-proton interactions or quadrupole pairing) have been made [10–15,37–41] to provide a theoretical basis for the signature inversion phenomenon

observed in odd-odd nuclei, a consistent picture is still lacking.

V. SUMMARY

This work presents a high-spin spectroscopic study of the neutron deficient nuclide ^{162}Ta . The level scheme of the nucleus was established up to a tentative spin and parity of $I^\pi = 30^-$ and a quasiparticle configuration assignment ($\pi h_{11/2} \nu i_{13/2}$) was made based on the observation of experimental alignments and Routhians together with a comparison of experimental $B(M1)/B(E2)$ ratios using the geometrical model of Dönau and Frauendorf. The phenomenon of signature inversion in Ta isotopes is shown to follow the same behavior as the Lu and Tm odd-odd isotones but with a more pronounced energy staggering. The reversal of the anomalous signature splitting above the paired band crossing observed in the $N \geq 91$ nuclides is absent for $N = 89$. This might be influenced by a different character of the S -band configuration below $N = 91$. The origin of signature inversion in odd-odd nuclei remains an important challenge for nuclear structure theory.

ACKNOWLEDGMENTS

The authors would like to thank the staff at the Accelerator Laboratory of the University of Jyväskylä for their excellent technical support. Support for this work was given by the Swedish Research Council, the Göran Gustafsson foundation, the Academy of Finland under the Finnish Centre of Excellence Programme 2006–2011 (Project No. 44875, Nuclear and Condensed Matter Physics Programme at JYFL), the UK Science and Technology Facilities Council and the European Union Fifth Framework Programme *Improving Human Potential—Access to Research Infrastructure* (Contract No. HPRI-CT-1999-00044), the Nordic Infrastructure support by NordForsk (Project 070315), and the Turkish Atomic Energy Authority (TAEK) under Project No. DPT-04K120100-4. We also acknowledge the support from the Finnish Academy (Contract No. 209430-111965). Additionally, we thank the EUROBALL owners committee (γ -pool network) and the UK/France (EPSRC/IN2P3) detector Loan Pool for providing the EUROGAM detectors of JUROGAM and GSI for the loan of two additional VEGA clover detectors.

-
- [1] D. G. Roux *et al.*, *Phys. Rev. C* **65**, 014308 (2001).
 - [2] D. G. Roux *et al.*, *Phys. Rev. C* **63**, 024303 (2001).
 - [3] K. Lagergren *et al.*, *Phys. Rev. C* **83**, 014313 (2011).
 - [4] M. Sandzelius *et al.*, *Phys. Rev. C* **80**, 054316 (2009).
 - [5] D. J. Hartley *et al.*, *Phys. Rev. C* **82**, 057302 (2010).
 - [6] Y. Z. Liu, Y. Ma, H. Yang, and S. Zhou, *Phys. Rev. C* **52**, 2514 (1995).
 - [7] L. L. Riedinger *et al.*, *Acta Phys. Pol. B* **32**, 2613 (2001).
 - [8] C. X. Yang and H. Y. Zhou, *Chin. Phys. Lett.* **20**, 2140 (2003).
 - [9] Y. H. Zhang, *Nucl. Phys. A* **834**, 32c (2010).
 - [10] R. Bengtsson *et al.*, *Nucl. Phys. A* **415**, 189 (1984).
 - [11] I. Hamamoto, *Phys. Lett. B* **235**, 221 (1990).
 - [12] P. B. Semmes and I. Ragnarsson, in *Proceedings: Nuclear Structure of Nineties* (Oak Ridge, TN, North-Holland, Amsterdam, 1990), p. 62.
 - [13] K. Hara and Y. Sun, *Nucl. Phys. A* **531**, 221 (1991).
 - [14] T. Komatsubara *et al.*, *Nucl. Phys. A* **557**, 419c (1993).
 - [15] F. R. Xu *et al.*, *Nucl. Phys. A* **669**, 119 (2000).
 - [16] C. W. Beausang and J. Simpson, *J. Phys. G* **22**, 527 (1996).
 - [17] M. Leino *et al.*, *Nucl. Instr. Meth.* **99**, 653 (1995).
 - [18] M. Leino, *Nucl. Instr. Meth. B* **126**, 320 (1997).
 - [19] R. D. Page *et al.*, *Nucl. Instr. Meth. B* **204**, 634 (2003).
 - [20] I. H. Lazarus *et al.*, *IEEE Trans. Nucl. Sci.* **48**, 567 (2001).
 - [21] P. Rahkila, *Nucl. Instr. Meth. A* **595**, 637 (2008).
 - [22] D. C. Radford, *Nucl. Instrum. Meth. A* **361**, 297 (1995).
 - [23] J. Simpson, private communication.
 - [24] H. Hübel *et al.*, *Z. Phys. A* **329**, 289 (1988).
 - [25] K. P. Blume *et al.*, *Nucl. Phys. A* **464**, 445 (1987).
 - [26] C. J. Gallagher and S. Moszkowski, *Phys. Rev.* **111**, 1282 (1958).
 - [27] X. Wang *et al.*, *Phys. Rev. C* **82**, 034315 (2010).
 - [28] M. A. Riley *et al.*, *Phys. Rev. C* **39**, 291 (1989).
 - [29] L. Yin *et al.*, *Eur. Phys. J. A* **11**, 379 (2001).
 - [30] S. M. Harris, *Phys. Rev.* **138**, B509 (1965).
 - [31] D. Dönau and S. Frauendorf, in *Proceedings: High Angular Momentum Properties of Nuclei*, edited by N. R. Johnson, (Harwood Academic, New York, 1983), p. 143.
 - [32] F. Dönau, *Nucl. Phys. A* **471**, 469 (1987).
 - [33] S. L. Gupta *et al.*, *Phys. Rev. C* **56**, 1281 (1997).
 - [34] M. A. Cardona *et al.*, *Phys. Rev. C* **56**, 707 (1997).
 - [35] S. André *et al.*, *Z. Phys. A* **333**, 247 (1989).
 - [36] R. F. Casten, *Nature Phys.* **2**, 811 (2006).
 - [37] B. Cederwall *et al.*, *Nucl. Phys. A* **542**, 454 (1992).
 - [38] A. K. Jain and A. Goel, *Phys. Lett. B* **277**, 233 (1992).
 - [39] N. Tajima, *Nucl. Phys. A* **572**, 365 (1994).
 - [40] N. Yoshida *et al.*, *Nucl. Phys. A* **567**, 17 (1994).
 - [41] Zheng Renrong, Zhu Shunquan, and Pu Yunwei, *Phys. Rev. C* **56**, 175 (1997).